# Staking lay-up effect on dynamic compression behaviour of E-Glass/epoxy composite materials: Experimental and numerical investigation

**Mostapha Tarfaoui[1,2*], Mourad Nachtane[1,3]**

[1] *ENSTA Bretagne, IRDL - UMR CNRS 6027, F-29200 Brest, France*
[2] *University of Dayton, Nanomaterials Laboratory, Dayton, OH 45469-0168, United States*
[3] *Laboratory for Renewable Energy and Dynamic Systems, FSAC - UH2C, Morocco*

*Corresponding author

DOI: 10.5185/amlett.2018.2060
www.vbripress.com/aml

## Abstract

Several industrial applications have exposed polymer matrix composite materials to a very high strain rate loading conditions, requiring an ability to understand and predict the material behaviour under these extreme conditions. Many composite aircraft structures such as fuselage, wing skins, engine nacelles and fan blades are situated such that impacts at high strain rates are a realistic threat. To investigate this threat, high velocity impact experiments and subsequent numerical analysis were performed in order to study the compressive loading of composite materials at high strain rates. Specimens are subjected with various orientations from low to high strain rates to determine the compressive material properties. Three fibre orientations such as: ±20°, ±60° and 90° of cubic geometry are tested in in-plane direction. The tests show a strong material sensitivity to dynamic loading and fibre direction. In the second part, the FEA results of the dynamic tests resulting in no damage appeared satisfactory. The FEA gives results which are in coherence with the experimental data. The improved understanding of these phenomena and the development of predictive tools is part of an ongoing effort to improve the long-term integrity of composite structures under dynamic loads. Copyright © VBRI Press.

**Keywords:** Composites, dynamic compression, experimental approach, finite element modelling.

## Introduction

Composites materials are becoming indispensable materials of todays because they offer a lot of benefits and they have many applications such as marine structure [1]. The most common innovative materials are polymer matrix composites (PMCs) consisting of a polymer (e.g., epoxy, polyester, urethane) matrix reinforced by thin diameter fibers (e.g., glass, graphite, aramids, boron) for the reason that found important applications in the shipbuilding industries and potential use in superstructures. The growing utilization of composites materials and innovations in material blends has approved composite component producers to meet the requirement for the military vehicle such as destroyers and aircraft carriers [3]. Characterizing the high strain rate response of the composite are essential for mechanical analysis.

Many researchers such as Powers and *al.* [4], Hosur and *al.* [5] performed high strain rate tests on composites with matrix polymer and indicated that the compressive strength of polymeric composites is sensitive to strain rate. The constitutive relations for orthotropic materials under dynamic loading are not readily attained and the mechanical properties must be defined experimentally over a large-scale range of strain-rates.

Although the difficulty of collecting reliable data is strengthened by problems confronted in the design and conducting impact tests on composites, the qualitative relationship between the dynamic response and the dynamic damage initiation and evolution for composite panels at high strain rates is still far from being sufficiently understood [6]. Important efforts have been made to examine the high strain rate behavior of more delicate materials such as composites and ceramics applying the split Hopkinson bar to measure dynamic response of materials under changing loading conditions [7-8]. Ochola *et al.* [9] studied the strain rate sensitivity of both carbon fibre reinforced polymer (CFRP) and glass fibre reinforced polymer (GFRP). Experimental results show that the dynamic composite strength for GFRP increases with increasing strain rates and the failure strain for both panels, CFRP and GFRP, is decreased with increasing strain rates. Vinson and Woldensenbet's [10] showed that the ultimate stress increases with increasing strain rate. The study conducted by Hosur *et al.* [] presents the effect of in-

 

plane off-axis testing of an 8-satin weave carbon fabric/SC15 composite panels. The specimens were experimentally tested in different fibre directions: 0°, 15°, 30°, 45°, 60°, 75°, and 90° with strain rates ranging from 1092 to 2425 s-1. From this study it was observed that the high strain rate of tested composites showed a considerable increase in the stress to failure and stiffness of the composite compared with the quasistatic loaded samples [11]. Depending on the fibre orientation, the ultimate strength and strain varied considerably and exhibited a nonlinear stress–strain behaviour that increased with angles up to 45°. Gary and Zhao [12] used low-impedance bars (nylon) to perform dynamic compression tests on glass epoxy panels. The failure strength of these panels is reported to be strain rate sensitive.

Recently, dynamic response and damage evaluation of laminate composites subjected to high strain rate loading conditions were analysed by Russo et al. (2017) with different temperature conditions, El Moumen *et al.* (2017) and Benyahia *et al.* (2017). From the experimental results, it appears that fibre orientation effects on dynamic responses and high strain rate properties. Tests were considered for a carbon epoxy system and carbon/nanotubes epoxy panels. Many different models [13-14] have been developed to predict failure stress and modes in composites subjected to quasi-static loading. However, few criteria have been developed and experimentally validated for high strain rate loading.

In this study, composite specimens of E-glass/epoxy composite were subjected to dynamic compression loading. Experimental tests were conducted with the help of split-Hopkinson pressure bar (SHPB). Samples were tested in in-plane (IP) direction. The fibre orientations of the samples were ±20°, ±60° and 90°. Stress-strain curves at increasing strain rates were obtained and analysed for different cases. The second part of this study consists with the modelling of the dynamic tests by using finite element method. The models are used for validating material characteristics and predicting their elastic behaviour.

## Experimental setup

### Materials

The material considered in this study is: 2400 Tex E-glass fibres impregnated with an epoxy polymer resin. The polymer is an EPOLAM pre-polymer, EPOLAM 2020 hardener and 2020 accelerator from Axson. The reinforcement architecture consists of a plain weave fabric with 90% in warp yarns and 10% in weft yarns. Composite panels were made using an infusion process with three different orientations namely: ±20°, ±60° and 90°. The composite specimens with dimension of 500×500 mm, were cut into cubic samples of the geometry dimensions as shown in **Table 1**.

**Table 1.** Geometry and fibre mass fraction of the samples, standard deviation in brackets.

| Panel | Thickness, (mm) | Surface ($mm^2$) | Void fraction (%) | Stacking sequence | Fibre volume Fraction (%) |
|---|---|---|---|---|---|
| A | 12.52 (0.3) | 13×13 (0.2) | 2.00 | $[\pm 20]_{20}$ | 54.0 (0.5) |
| B | 13.00 (0.1) | 13×13 (0.2) | 1.78 | $[\pm 60]_{20}$ | 55.0 (0.5) |
| C | 13.00 (0.1) | 13×13 (0.2) | 2.26 | $[90]_{40}$ | 53.5 (0.5) |

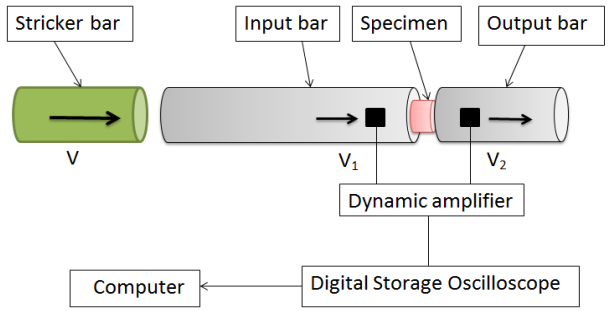


**Fig.1.** Typical compressive split Hopkinson bar apparatus.

### Testing method

The split Hopkinson pressure bar is one of the most technique for identifying the dynamic response of materials and defining material properties as high strain rates [15-16]. The schematic representation of Hopkinson bars is given in **Fig. 1**.

The dynamic compression test conducted in this study consists in placing cubic specimens with 13mm in length between two bars with a high elastic limit, called input and output bars. The diameter of bars was 20mm and the striker bar was 0.8m long, while the incident bar length was 3m and 2m for transmitted bar. These bars are correctly aligned and are able to slide freely on their support. The impacted specimen is not attached to the bar in order to prevent the perturbations of measurements due to additional interfaces[17]. The experimental set-up consists of (1) a stress generating system which is comprised of a Hopkinson bars and the striker, (2) a composite specimen and (3) a stress measuring system made up of sensors (typically, resistance strain gauges) and (4) a data acquisition system. The signals, obtained during impact test are treated with Maple Software using Fast Fourier Transformation in order to obtain the evolution of the dynamic behaviour as: stress vs. strain, strain rate vs. time, incident and transmitted load and velocity at the interfaces input bar/sample and output bar/sample vs. time.

All of the specimens [±20]20, [±60]20 and [90] 40 were impacted with impact pressures 0.5, 0.6, 0.7, 0.8, 0.9, 1.0, 1.2, 1.4 and 1.6 bar in the in-plane loading direction. A typical signal of incident, reflected, and transmitted bars measured from strain gauges and recorded by the digital oscilloscope at the strain rate of 831 s-1 test is shown in **Fig. 2**.

 

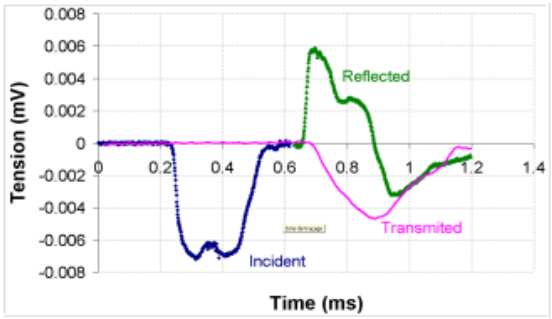


**Fig. 2.** Example of incident, reflected and transmitted pulse, P=0.9 bar (831 s-1).

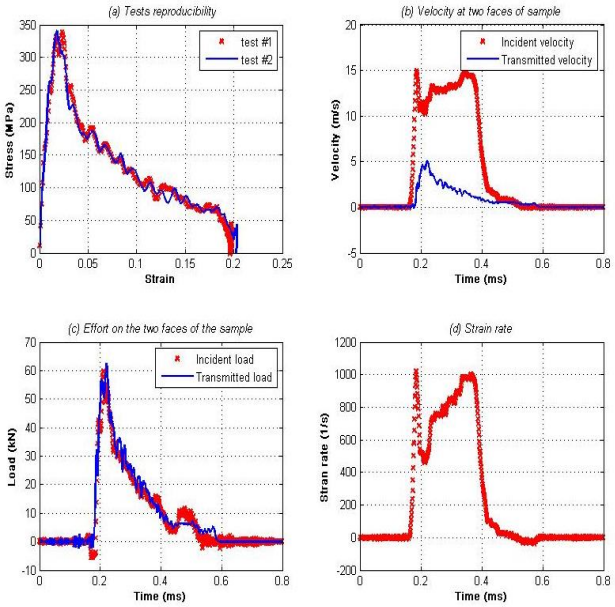


**Fig. 3.** Typical experimental signal of FFT analysis, P=1.2 bar.

## Experimental results

In order to ensure the reproducibility of tests a minimum of three tests were carried out with the same impact pressure. **Fig. 3** shows an example of experimental data processing obtained during impact with Hopkinson bars. From these curves it is noted that the tests are repeatable and a fact that was checked for each test.

It should be mention that the strain rate evolution is sensitive to the entry pressure P in the chamber of compressed air, the loading direction and the sample lay-up. **Fig. 4** shows the variation of the strain rate vs. time of [±20]20, [±60]20 and [90]40 for 9 impact pressures. The presence of a second peak, in the experimental signals, is the principal characteristic of these curves, which characterizes the onset of macroscopic damage, which is detailed in [18-19].

The experimental behaviour, under dynamic compression, for IP tests is dominated by compressive properties of the polymeric resin and the damage initiation and damage kinetics throughout specimens are two affected by the orientation of fibre. It should be noted that for non-damaging tests, the curve of the strain rate does not presnt a second peak and its decay passes through negative values characteristic of the springback behaviour of the specimens. **Fig. 5** shows the stress-strain curves for different cases. The combination of **Fig. 4** and **Fig. 5** reveals that the second peak, appeared in curves of **Fig. 4**, corresponds to the fall of stress **(Fig. 5)** in the sample. For the case of [90]40 composite laminate, a brittle behaviour is observed, which is controlled by epoxy polymer failure. According to the various fibres orientations, the nonlinear part of the curves is different and corresponds to different damaging modes obtained in the specimens.

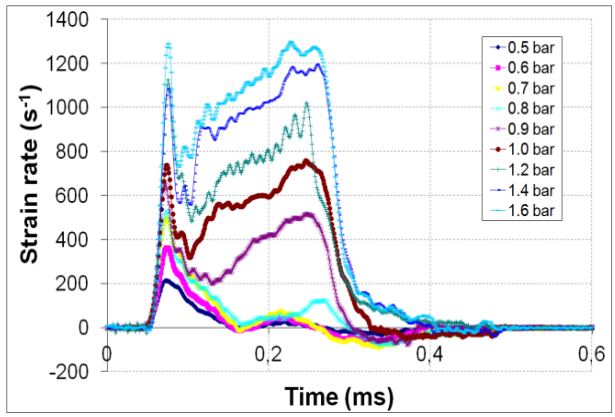


(a) $[\pm 20]_{20}$

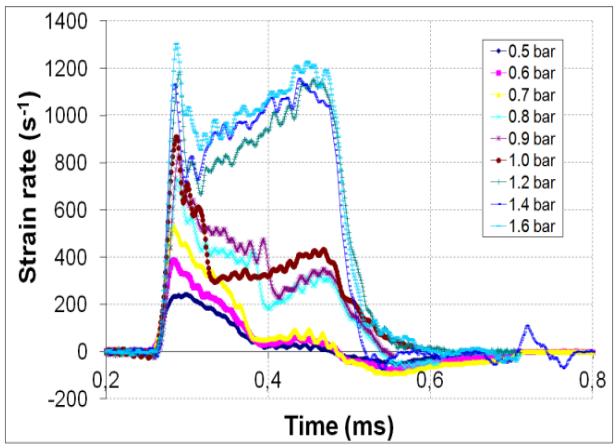


(b) $[\pm 60]_{20}$

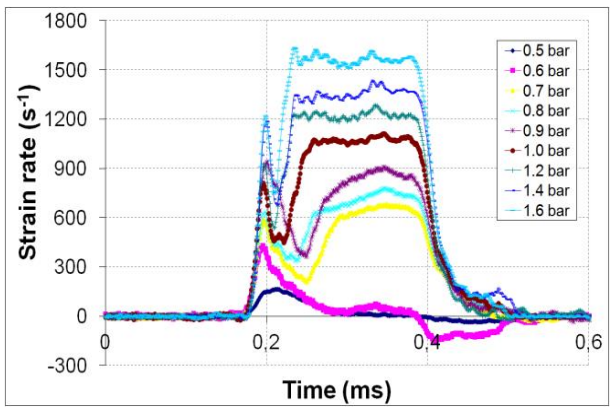


(c) $[90]_{40}$

**Fig. 4.** Strain rate variation as a function of different impact pressure.

 

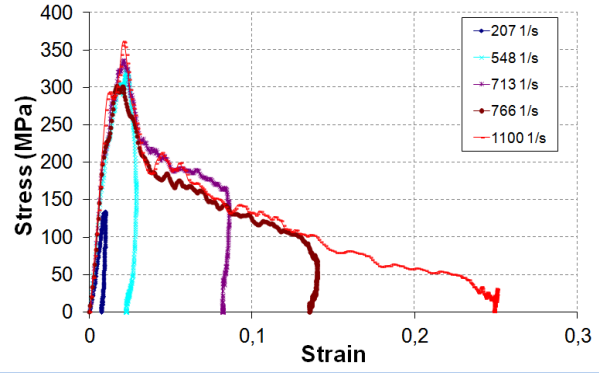


(a) $[\pm 20]_{20}$

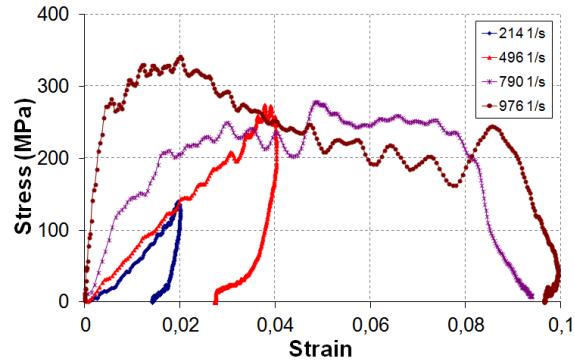


(b) $[\pm 60]_{20}$

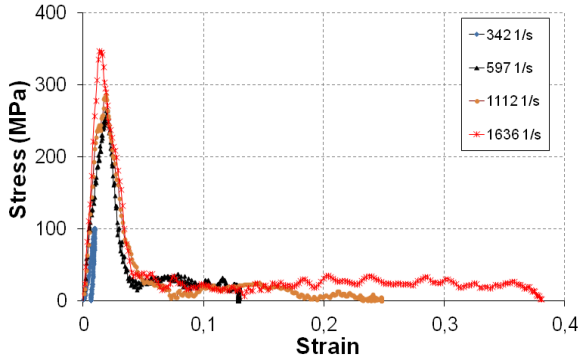


(c) $[90]_{40}$

**Fig. 5.** Stress - strain curve evolution versus strain rate.

## Finite element analysis

### *Numerical model, meshing and contact algorithm*

Experimental setup of the dynamic behaviour of glass epoxy composite was detailed. In this section the numerical modelling of these tests are given. Abaqus software was used to simulate the compression tests of composite specimens [20]. Based on microscopic observations, the composite specimen was modeled as solid laminated elements with transversely isotropic plies. The bars (input, output bars and impactor), of great stiffness (quenched steel) compared to the composite specimen, was modeled as deformable body and the surfaces in contact with the specimen were taken as the "master surface". Modeling as deformable body requires a 3D elements which generates a very important computing time. The potential contact area of the specimen was taken as a "slave surface" so the individual nodes of the composite were constrained not to penetrate the surfaces of the bars. The relative motions of the contact surfaces were modeled as "small sliding", which assumes that contact surfaces do not move very much relative to each other. The contact algorithm used is based on the penalty method. Hexahedral solid elements with reduced integration C3D8R is considered for specimen meshing. Meshes consist of isometric elements. For these two types of elements, five integration points are considered in the thickness of each layer. The integration method uses the Simpson rule. The selected elements have linear interpolation. They give better results for modeling contact and impact with the possibility of severe distortions of the elements.

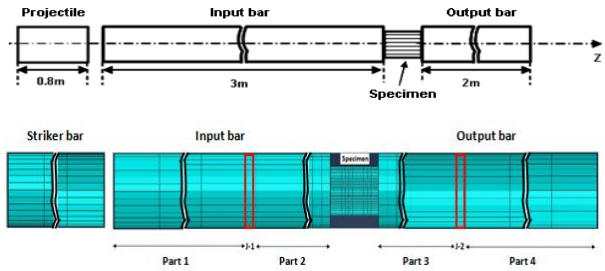


**Fig. 6.** Full model (FM) with striker bar.

A sketch of the model is presented in **Fig. 6** with associate mesh. The projectile, the bars and the specimen are modelled as deformable bodies. Note that the mesh used is as follows: 1mm meshes size of the sample; 13mm mesh size of the striker, mesh of the cross-section of the bars: 8 elements for the diameter and 24 of the perimeter. For mesh parts, we have: Parts 1 and 4: coarse mesh of 13mm and Parts 2 and 3: biased mesh (refined in the direction of the sample: 150 elements with a ratio of 5).

The different physical quantities analysed, see **Fig. 7** and **Fig. 8**, and compared with experimental results are:

- $F_i$ and $F_t$ : incident and transmitted loads applied to the sample, interfaces Input bar/sample/Output bar,
- $V_i$ and $V_t$ : the incident and transmitted velocity,
- Incident ($J_1$) and transmitted ($J_2$) Strain of the bar at the location of the two gauges.

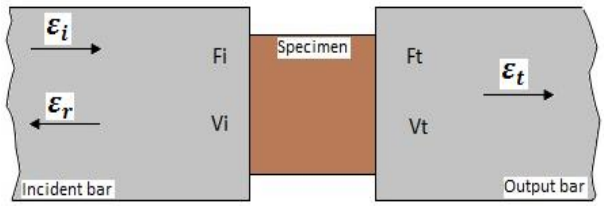


**Fig. 7.** Different physical quantities of the model.

 

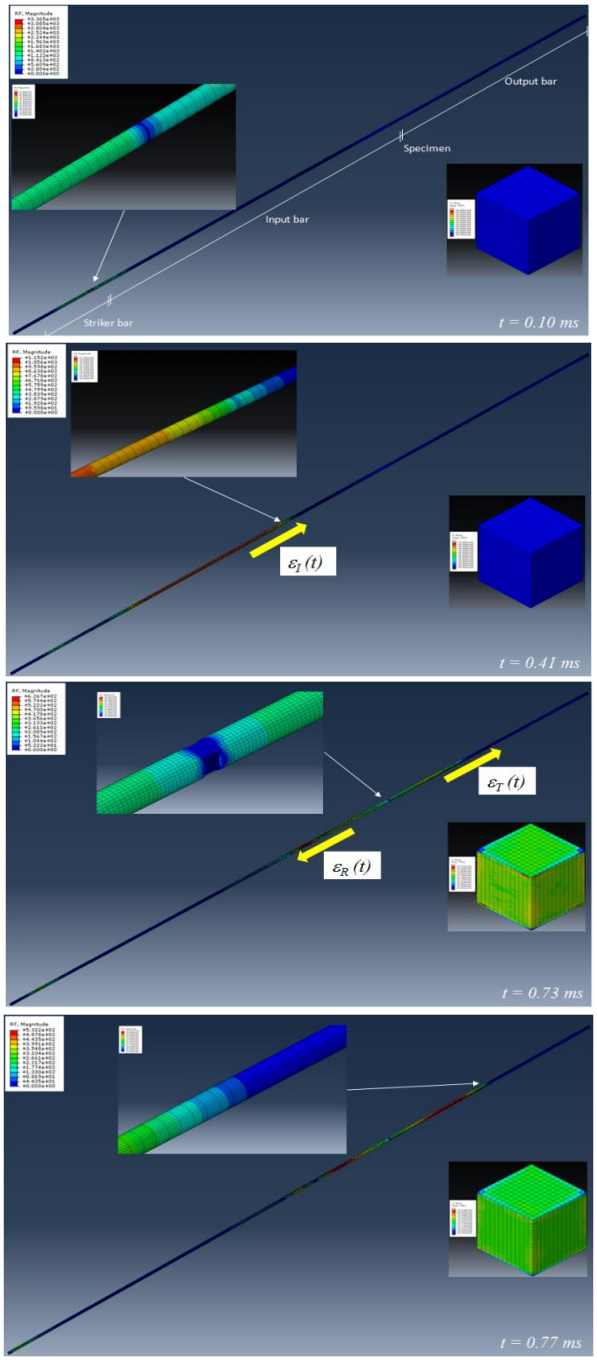


**Fig. 8.** Dynamic compression test – FEA.

## Results and discussion

**Figs. 9, 10, 11** and **12** show a comparison between the experimental data and the results of numerical model. This comparison shows a good correlation for the different orientations. The following results are obtained:

- For the strain of incident and reflected compression wave measured by the gauge J1, the numerical model presents a good estimation compared with experimental results. A small difference is observed can be linked with velocity of the impactor in numerical model. The latter is estimated from the average value given by the incident gauge signal.

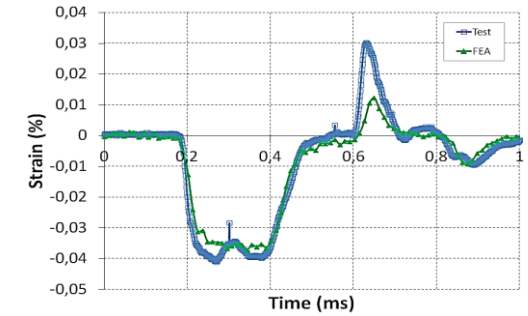


(a) Strain at $J_1$

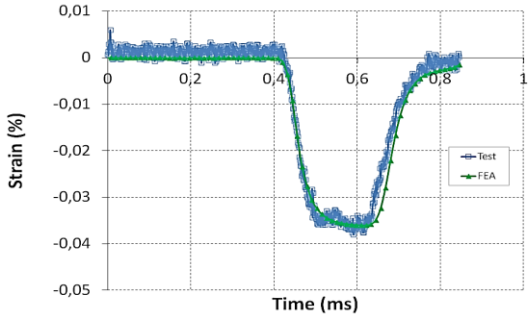


(b) Strain at $J_2$

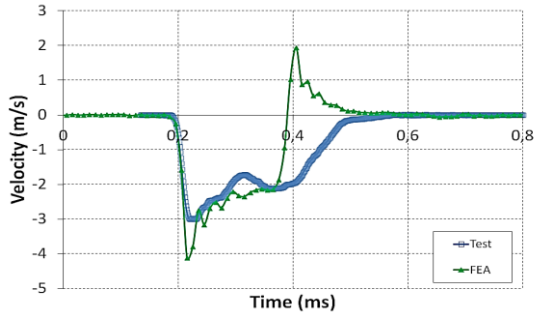


(c) Incident velocity

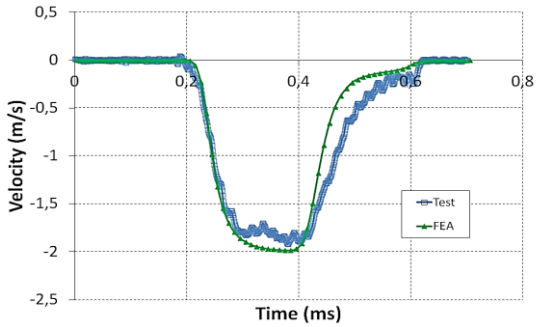


(d) Transmitted velocity

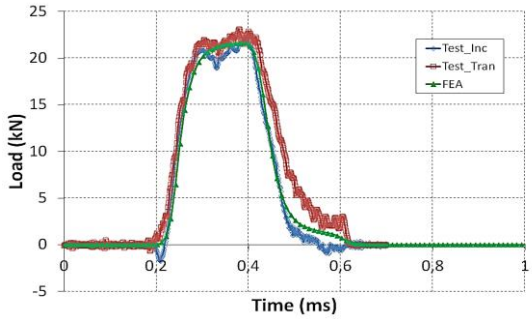


(e) Load vs. displacement

**Fig. 9.** Correlation experimental/numerical results, IP test $[\pm 20]_{20}$, P = 0.5 bar.

- The correlation of the transmitted strain reveals a good agreement. It should be noted that the absence of the damper bar in the global model causes multiple reflections where the presence of a tensile wave of the same amplitude.
- For the incident velocity, an adequate relationship in the first part of the curve is observed, but the second part shows a divergence. Actually, as the numerical velocity is used at the incident surface of the bar in contact with the specimen, one has many reflections of the wave which produce overlapping velocities of opposite signs.
- The transmitted numerical velocity gives a good approximation with the experimental results.
- The evolution of the incident and transmitted loads, given at two interfaces of the bars in contact with the specimen are well simulated. We have observed the same level of the maximum load and the same rise and fall of the load. At the experimental results, we find a negligible deviation between the incident and transmitted load that may be compared to the experimental requirements: the shape of the specimens is not correctly cubic.

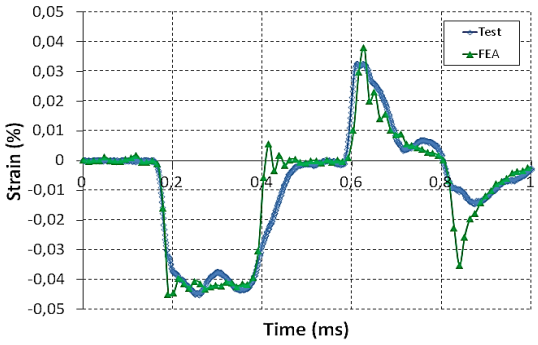


(a) Strain at $J_1$

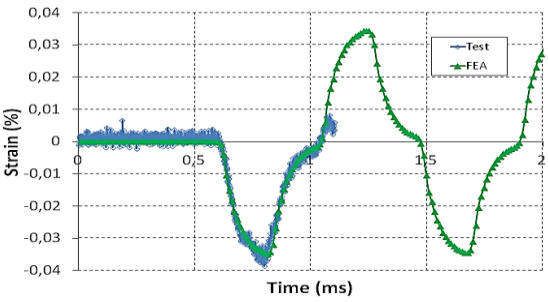


(b) Strain at $J_2$

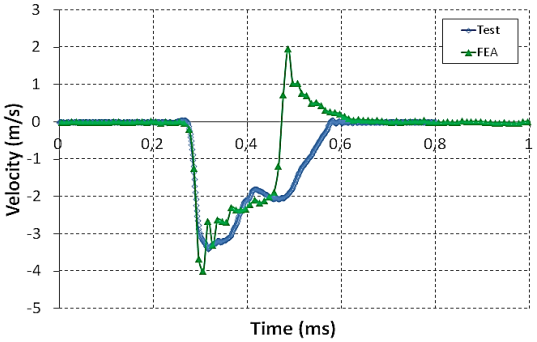


(c) Incident velocity

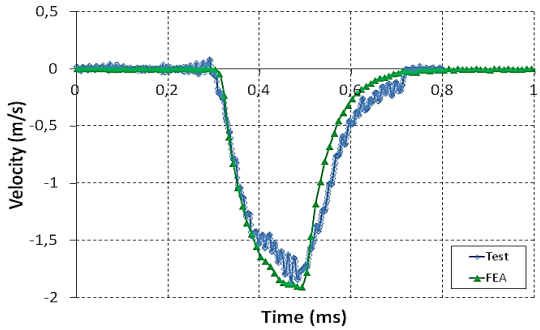


(d) Transmitted velocity

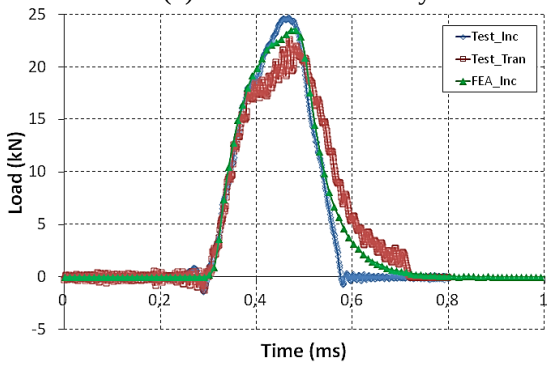


(e) Load vs. displacement

**Fig.10.** Correlation experimental/numerical results, IP test $[\pm 60]_{20}$, P = 0.5 bar

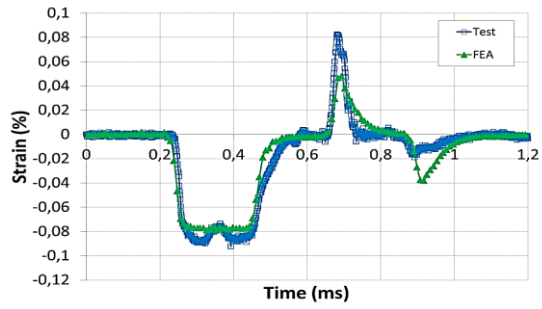


(a) Strain at $J_1$

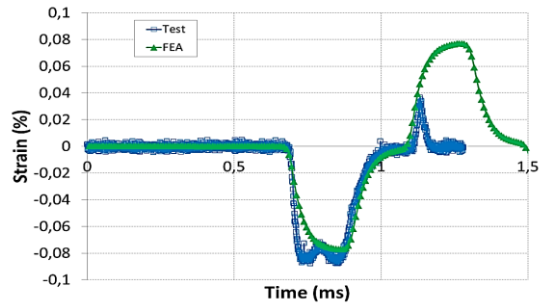


(b) Strain at $J_2$

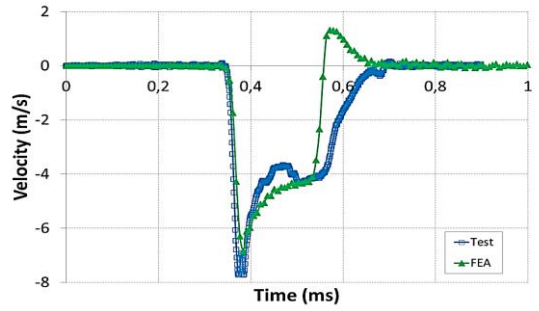


(c) Incident velocity

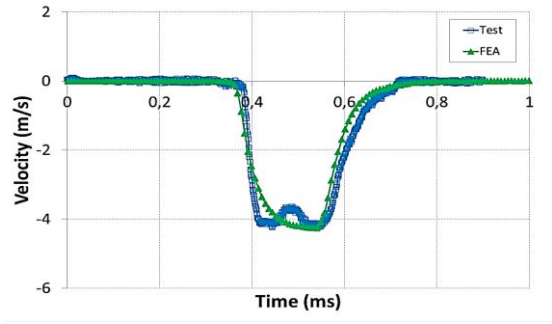


(d) Transmitted velocity

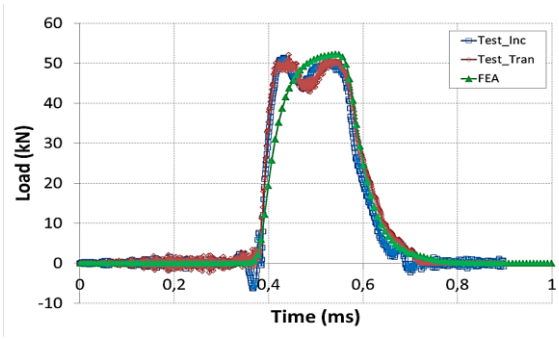


(e) Load vs. displacement

**Fig. 11.** Correlation experimental/numerical results, IP test $[\pm 90]_{40}$, P=0.6 bar.

## Conclusion

In this research, we performed an experimental and numerical study of the high strain rate response of composite specimens for different fibres orientations [± 20]20, [± 60]20 and [90]40 using a Split Hopkinson pressure bar (SHPB). Firstly, for the small pressure ranges there was no macroscopic damage, but the existence of microscopic damage remains a possibility. It can also be noted that the orientation of the laminates is a major parameter for improving the resistance to dynamic compression. On the other hand, the kinetics of the damage for the in-plane loading is strictly conditioned by the orientations of the fibers of the sample. The initiation and propagation of failure mechanisms at different stress levels were examined. Finally a numerical model was built in Abaqus software and compared with experimental curves. A good agreement between numerical results and experimental data is observed.

### References


1. Mourad, N., Mostapha, T., & Dennoun, S.; Promotion of Renewable Marines Energies in Morocco: Perspectives and Strategies. Wor Acad of Sci, Engin and Techn Intern Jour of Ene and Pow Engin. **DOI:** 10.1999/1307-6892/76700
2. Nachtane, M., Tarfaoui, M., El Moumen, A. & Saifaoui, D; Comp Stru, 2017, 170, 146-157. **DOI:** 10.1016/j.compstruct.2017.03.015
3. Nachtane, M., Tarfaoui, M., Saifaoui, D., El Moumen, A., Hassoon, O. H., & Benyahia, H. (2018); Egy Rep. **DOI:** 10.1016/j.egyr.2018.01.002
4. Tsai J., Sun C.T.; Intern Jour of Sol and Stru. **DOI:** 10.1016/j.ijsolstr.2003.12.010
5. El Moumen, A., Tarfaoui, M., Hassoon, O., Lafdi, K., Benyahia, H., & Nachtane, M.; Appli Comp Materi. **DOI:** 10.1007/s10443-017-9622-8
6. Hassoon, O. H., Tarfaoui, M., El Moumen, A., Benyahia, H., & Nachtane, Appl Comp Mater. **DOI:** 10.1007/s10443-017-9646-0
7. Hosur MV, Alexander J, Vaidya UK, Jeslani S, Mayer A.; Comp and Stru. **DOI:** 10.1016/S0263-8223(03)00134-X
8. Tsai J.L. and Sun C.T.; Comp Scie and Techn. **DOI:** 10.1016/j.compscitech.2005.01.013
9. Gueraiche L.,Tarfaoui M.,Ossmani H.&El Malki A.; Comp Struct **DOI:** 10.1016/j.compstruct.2015.02.061
10. Nachtane, M., Tarfaoui, M., & Saifaoui, D.; Matériaux composites pour les énergies marines renouvelables. Éditions universitaires européennes. ISBN: 978-620-2-26157-9
11. Ochola R.O., K.Marcus, G.N. Nurick and T.Franz.; Comp Stru, **DOI:** 10.1016/S0263-8223(03)00194-6
12. Vinson J., E ; Woldesenbet.; Journ of Comp Mater **DOI:** 10.1177/002199801772662136
13. Tarfaoui, M., Nachtane, M., Khadimallah, H., & Saifaoui, D.; Appl Comp Mater. **DOI:** 10.1007/s10443-017-9612-x
14. Gotsis P.K., Chamis C.C. & Minnetyan L.Compo Scie &Techn. **DOI:** 10.1016/S0266-3538(02)00095-7
15. Gary G. and H. Zhao.; Comp Part A: Appli Scie and Manufa, **DOI:** 10.1016/S1359-835X(00)00026-9
16. El Moumen, A., Tarfaoui, M., & Lafdi, K.; Compo Part B: Engin. **DOI:** 10.1016/j.compositesb.2017.02.005
17. Arbaoui, J., Tarfaoui, M., & Alaoui, A. E. M. (2016). Internl Jour of Imp Engin. **DOI:** 10.1177/1056789516651691
18. Shah, O. R., & Tarfaoui, M. (2016). CompoPart B: Engin, **DOI:** 10.1016/j.compositesb.2016.04.042
19. Tarfaoui, M., Nême, A., & Choukri, S.(2009). Journ of comp mater. **DOI:** 10.1177/0021998308098336
20. Abaqus 6.14: Analysis User's Manual.


 